Hindawi
Advances in High Energy Physics
Volume 2022, Article ID 5482034, 11 pages
https://doi.org/10.1155/2022/5482034

Research Article

Model Comparison of the Transverse Momentum Spectra of Charged Hadrons Produced in $PbPb$ Collision at $\sqrt{s_{NN}} = 5.02\,\mathrm{TeV}$

Rohit Gupta and Satyajit Jena

Department of Physical Sciences, Indian Institute of Science Education and Research (IISER) Mohali, Sector 81, S.A.S., Nagar, Punjab 140306, India

Correspondence should be addressed to Satyajit Jena; sjena@iisermohali.ac.in

Received 21 October 2021; Revised 14 March 2022; Accepted 31 May 2022; Published 14 June 2022

Academic Editor: Carlos Pajares

Transverse momentum, p_T, spectra are of prime importance in order to extract crucial information about the evolution dynamics of the system of particles produced in the collider experiments. In this work, the transverse momentum spectra of charged hadrons produced in $PbPb$ collision at 5.02 TeV have been analyzed using different distribution functions in order to gain strong insight into the information that can be extracted from the spectra. We have also discussed the applicability of the unified statistical framework on the spectra of charged hadron at 5.02 TeV

1. Introduction

The quest to develop the understanding of Quantum Chromodynamics (QCD) matter created during the very early universe has been the primary motivation behind several theoretical as well as experimental studies in particle physics. Whether the QCD phase transition is first order, second order, or simple crossover and what are the critical temperature and the order parameters of phase transition, etc., are some of the long-standing questions that intrigue the researchers to explore QCD phase diagram by utilizing data from different heavy-ion collider experiments like Relativistic Heavy Ion Collider (RHIC) at BNL and in Large Hadron Collider (LHC) at CERN. The QCD matter under discussion is popularly known as Quark-Gluon Plasma (QGP) which cooks up under extreme conditions of temperature and energy density. When the temperature (T) and the energy density (ε) reach a critical value, quarks no longer remain confined inside their individual hadron and instead become free to move over a nuclear volume forming a deconfined QGP state. Such extreme condition has been achieved by colliding heavy ions moving at the ultrarelativistic speed in the experiments at RHIC and LHC and provided us the tool to investigate and to uncover the mystery of the fireball that filled our universe few microseconds after the Big Bang.

The theoretical reasoning behind the formation of QGP comes from the asymptotic freedom due to the nature of the running coupling strength of constituent partons. The theory of quark gluon interaction, QCD, dictates that the coupling strength between quarks and gluons increases with a decrease in the energy scales (or increase in length scale). On the other hand, the length scale can be decreased by bringing partons closer to each other. As the length scale reduces, the coupling strength also decreases, and it reaches a point where quarks and gluons asymptotically appear to be free from their nucleonic volume changing its hadronic degrees of freedom to partonic degrees of freedom. Hence, a dense hot soup of quarks and gluons forms, which we call QGP. This is exactly what experiments like RHIC and LHC had achieved by colliding highly energetic nucleons travelling at ultrarelativistic speed. However, the time scale of such process is extremely small so it is not possible to directly probe and characterize it using present day technologies. In experiments, we only receive the information about kinematics of final state particles that are free streaming to the detectors. We utilize the kinematics of these final state particles to get information about the underlying process that led to the formation of these particles.

The transverse momentum, p_T, spectra of final state particle are a crucial kinematic observable that can be utilized as an effective probe to understand the thermodynamical properties of the system produced in the collision. It is also an essential observable to understand the dynamics of QGP and the quark-hadron phase transition. Several theoretical models [1–4] have been developed to characterize p_T spectra and to extract different physical parameters that can be further used to enhance our understanding of the system produced during such collisions. Most of these models are developed based on the statistical and thermodynamical approach since it is almost impossible to apply perturbative field theory calculations because of the high QCD coupling strength at low p_T (due to asymptotic freedom).

In this work, we have performed a comparative study of different models on p_T spectra of charged hadrons produced in *PbPb* collision at the recently published result at $\sqrt{s_{NN}} = 5.02$ TeV [5] along with the 2.76 TeV [6] data measured by the ALICE experiment at CERN.

2. Models

As discussed in the previous section, it is difficult to apply perturbative QCD at low-p_T region of spectra as the coupling strength becomes extremely high at a low momentum transfer scale. Hence, we rely on the phenomenological models. Among several such models, statistical thermal approaches are widely used to explain transverse momentum spectra. Initial work by Koppe [7, 8], Fermi [9, 10], and Hagedorn [11, 12] developed the fundamentals of the statistical description of particle spectra in high energy physics. These initial works were followed by several applications of statistical thermodynamics in studying the particle production mechanism using the momenta carried out by outgoing particles. In this section, we will discuss different models developed to explain the spectra, and we will present the results obtained by fitting the p_T spectra data produced in 5.02 TeV collision. Some of the models discussed below require the information of mass of the constituent particle. Since a larger contribution of charged hadrons comes from pion (~ 70%), we have used the mass of pion while analyzing the spectra of charged hadrons.

2.1. Boltzmann Distribution. For a system that is considered to be of purely thermal origin, the most natural choice to explain the statistical distribution of the energy of constituent particles is the standard Boltzmann-Gibbs statistics. Boltzmann distribution has long been used to explain energy spectra [1, 13] of the classical statistical system. Because the temperature of the system during heavy-ion collision is extremely high and Fermi-Dirac and Bose-Einstein statistics approach Maxwell-Boltzmann statistics at high temperature, we can use Boltzmann distribution to explain the spectra of particles produced during the heavy-ion collision. In the case of Boltzmann distribution, we can write number density as [1, 13]

$$\frac{d^2N}{2\pi p_T dp_T dy} = m_T \frac{gV}{(2\pi)^3} \exp\left(\frac{-m_T}{T}\right). \quad (1)$$

Here, m_T is the transverse mass and is related to transverse momentum by $m_T = \sqrt{m^2 + p_T^2}$, g is the spin degeneracy factor, and V is volume of the system under consideration. In Figure 1, we have fitted the p_T spectra of charged hadrons that produced *PbPb* collision at 5.02 TeV with the Boltzmann distribution function (Equation (1)). We observe that the data deviate significantly from the BG function at low and high p_T regions of the spectra. This deviation finds its origin in the low number of particles in the collision. BG statistics apply to the system where the number of particles in the system should be of the order of the Avogadro number; however, only a few thousand particles are produced in heavy-ion collision. At the same time, the applicability of BG statistics is limited to the system where entropy of the ensemble is extensive as well as additive in nature. To tackle these fundamental issues, we need to find a solution for nonextensive formalism which can be applied to the system under discussion. Therefore, a generalization of BG statistics was proposed by Tsallis in his seminal work in Ref. [2] to tackle nonextensivity in the system. By doing so, it overcomes the limitation of BG statistics. In this context, we provide a brief discussion on Tsallis statistics and the corresponding fit result of *PbPb* collision at $\sqrt{s_{NN}} = 5.02$ TeV.

2.2. Tsallis Distribution. To provide a generalized formalism to explain nonextensive systems such as the system produced in the heavy-ion collision, Tsallis statistics, also known as nonextensive statistics, were proposed as a generalization of Boltzmann-Gibbs statistics in 1988 by C. Tsallis. In Tsallis statistics, a parameter $'q'$ has been introduced, which takes care of the nonextensivity in the system. This new parameter also acts as a scaling factor for the number of particles to make this statistic applicable to the system with a low number of particles compared to the Avogadro number. Here, normal exponential is replaced by q-exponential as

$$\exp_q(x) = [1 - (q-1)x]^{-1/q-1}, \quad (2)$$

which in the limit $q \longrightarrow 1$ gives us normal exponential.

Further, entropy in the case of Tsallis statistics [2] is given as

$$S_q = k\frac{1 - \sum_i p_i^q}{q-1}. \quad (3)$$

The functional form of transverse momentum spectra in the case of Tsallis statistics can be obtained by replacing normal exponential in Equation (1) with q-exponential:

$$\frac{1}{2\pi p_T}\frac{d^2N}{dp_T dy} = \frac{gVm_T}{(2\pi)^3}\left[1 + (q-1)\frac{m_T}{T}\right]^{-q/q-1}. \quad (4)$$

This distribution function converges to Boltzmann distribution in the limit $q \longrightarrow 1$. Also, Tsallis statistics have been proved to be thermodynamically consistent following

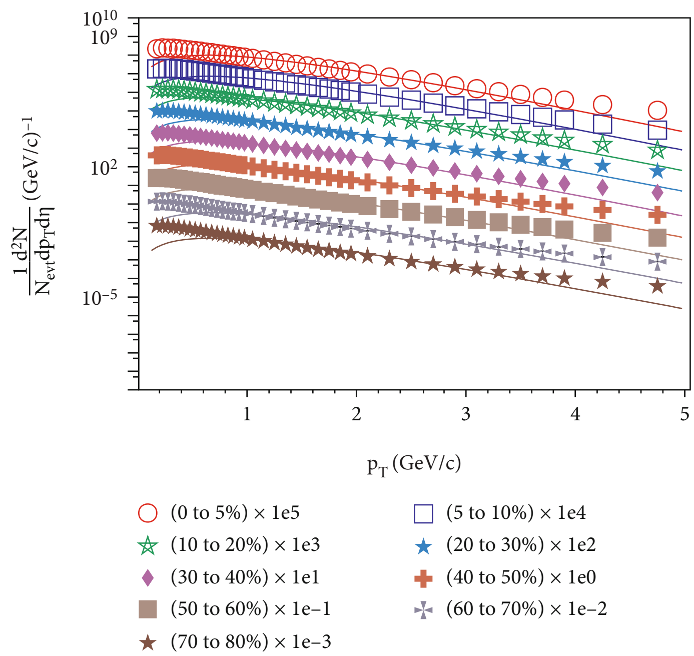

FIGURE 1: The transverse momentum spectra of charged hadrons at different centralities produced at collision energies of 5.02 TeV [5] fitted with Boltzmann (Equation (1)).

the laws of thermodynamics [14]. This form of transverse momentum spectra has been shown in different works [14–18] to nicely explain the spectra in a limited p_T region. Additionally, it has been observed that there are certain systems [19] with significant long-range interactions; the entropy in such system can be nonadditive and nonextensive, and the Tsallis formalism has been used to explain such system [20].

Figure 2 shows the fitting of Tsallis distribution to the p_T spectra of charged particles produced in *PbPb* collision at $\sqrt{s_{NN}} = 5.02$ TeV. It is evident from the figure that Tsallis distribution provides a much better fit to the spectra compared to the Boltzmann distribution. The detailed comparison of χ^2/NDF values is given in Table 1; we can observe that there is a significant improvement in explaining the spectra of *PbPb* collision at $\sqrt{s_{NN}} = 5.02$ TeV.

However, we observed that it does not explain the data at low and high p_T part of spectra. This might be due to the various particle production mechanisms in the heavy-ion collision, affecting the nature of spectra. Therefore, the applicability of Tsallis statistics is only limited to soft p_T regimes of the spectra (although it deviates narrowly at low p_T) whereas for high p_T, dominated by hard processes, it does not explain. As shown and discussed in Ref. [21–23], the Tsallis formalism becomes extremely complex to incorporate hard processes, and eventually, a modification is required to explain very high p_T part of the particle spectra. On the contrary, the particle production is dominated by hard QCD processes at the high p_T region of the spectra, which could be explained by a QCD-inspired power law form of function such as

$$f(p_T) = \frac{1}{N}\frac{dN}{dp_T} = Ap_T\left(1 + \frac{p_T}{p_0}\right)^{-n}. \tag{5}$$

A unified model to explain the contribution of both soft and hard processes to p_T spectra is still an open problem. Before we discuss the unified formalism [24, 25], we would like to discuss several other approaches to explain p_T spectra. Apart from the purely statistical models discussed above, several hydrodynamics-based models are also developed to explain the spectra considering the initial state fluctuation and the collective behaviour of the QCD matter created during the collision.

2.3. Blast-Wave (BW). It is experimentally established that the system produced during the high energy collision has an azimuthal anisotropy because of the difference in flow velocities along different directions. This azimuthal anisotropy is a result of some initial state geometrical effects that arise during the collision. Thus, it can be argued that the outgoing particles must carry the imprint of such effects and can influence the nature of the spectra. To incorporate such effects on spectra, several models are proposed [3, 4]. The Blast-Wave model is a hydrodynamics-inspired model developed to include the flow properties along with the random thermal motion of particles in order to give a complete picture of the evolution dynamics of QGP, including the azimuthal anisotropy. Transverse momentum spectra in the case of the Blast-Wave model [3] are given as

$$\frac{dN}{p_T dp_T} \propto \int_0^R r\, dr m_T I_0\left(\frac{p_T \sinh \rho(r)}{T_{\text{kin}}}\right) \times K_1\left(\frac{m_T \cosh \rho(r)}{T_{\text{kin}}}\right). \tag{6}$$

Here, m_T is the transverse mass and I_0 and K are modified Bessel functions. Also, $\rho(r) = \tan h^{-1}\beta$ and β is the

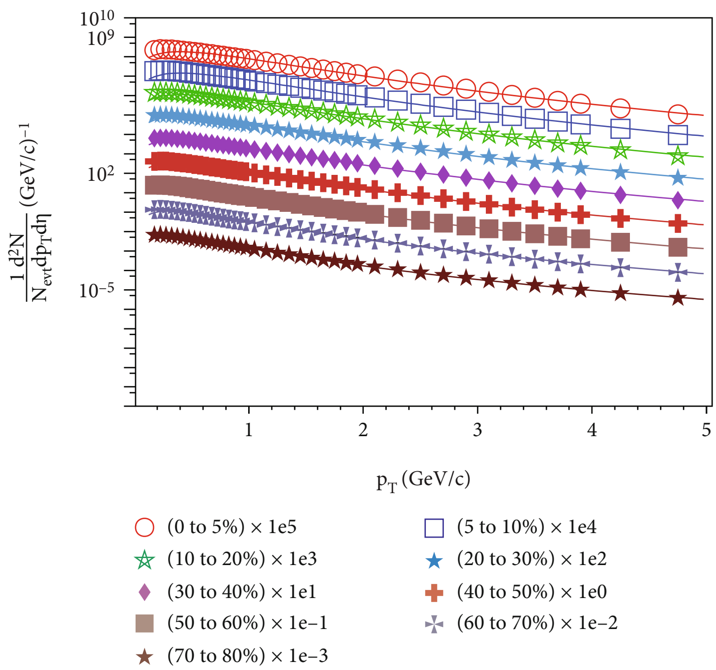

FIGURE 2: The transverse momentum spectra of charged hadrons at different centralities produced at collision energies of 5.02 TeV [5] fitted with Tsallis (Equation (4)).

transverse radial flow velocity which is parameterized in the form of a power law of the form $\beta_t(r) = \beta_s(r/R)^n$, where β_s represent the surface flow velocity and n is the exponent of the flow profile. The average transverse flow velocity ($\langle\beta_T\rangle$) is given in terms of β_s and exponent n as $\langle\beta_T\rangle = \beta_s \times 2/2 + n$ [3]. Finally, r/R represents the radial position of the thermal source.

The temperature extracted using the BW function has a different interpretation as compared to the temperature extracted from the Boltzmann-Gibbs function (Equation (1)) or Tsallis function (Equation (4)). Fitting with BW function gives us kinetic freeze-out temperature (T_{kin}) whereas fitting with BG or Tsallis distribution gives us effective temperature (T_{eff}). These two quantities are related as [26]

$$T_{\text{eff}} = T_{\text{kin}} + f(\beta_t). \quad (7)$$

Here, $f(\beta_t)$ is a function of transverse flow velocity β_t.

We show the result of Blast-Wave fitting to the p_T spectra of particles produced in 5.02 TeV collision in Figure 3. The fitting yields the kinetic temperature as 113.6 MeV and the average flow velocity close to 0.63c for most central collision. The χ^2/NDF values are close to unity for central collisions, but they start to increase with the decrease in the nuclear overlap by approaching a value of 20 for most peripheral collisions. This formalism does not include the concept of nonextensive; therefore, a generalization of the Blast-Wave model to include a nonextensive system is discussed in the next section.

2.4. Tsallis Blast-Wave (TBW). The Tsallis Blast-Wave method is an extension of the Blast-Wave method which was introduced to take into account the effect of nonextensivity in the system along with the flow properties. As discussed elsewhere in the article, Tsallis formalism can be used to tackle the system with nonextensivity; the Boltzmann distribution used in the Blast-Wave model is replaced by the Tsallis distribution in order to get the Tsallis Blast-Wave function [3, 4]. Transverse momentum spectra in the case of TBW are given as

$$\frac{dN}{p_T dp_T} \propto m_T \int_{-Y}^{Y} \cos h(y)\, dy \int_{-\pi}^{\pi} d\phi \int_{0}^{R} r dr \times \left(1 + \frac{q-1}{T}\left(m_T \cos h(y) \cosh(\rho) - p_T \sin h(\rho) \cos\phi\right)\right)^{-1/q-1}. \quad (8)$$

Here, y represent rapidity and ρ is the flow profile as described in Blast-Wave (BW).

After its introduction, the TBW method has been used in different works to fit p_T spectra of particles and extract information related to the thermodynamics and hydrodynamics evolution of the system produced in the heavy-ion collision. For TBW fit, the value of n is set to one [3, 4].

We have shown the fitting of p_T spectra with TBW function in Figure 4. The value of kinetic freeze-out temperature extracted from the TBW fit shows a declining trend with the increase in centrality, and the average flow velocity is around 0.4c. The TBW model gives a holistic view of particle production in high energy collision, including statistical and hydrodynamical description but only at the low p_T part of the spectra. Although the result obtained by this method gives a better explanation at low p_T, it does not take care of hardness in the spectra in the high p_T region, which is dominated by the particles produced in hard scattering processes.

Table 1: Table of parameter values obtained after fitting charged hadron spectra at 3 different centralities with different functions.

Variable	Method	Energy (TeV)	0 to 5%	40 to 50%	70 to 80%
T_{eff} (MeV)	BG	2.76	316.95 ± 2.74	316.3 ± 3.58	305.23 ± 5.75
		5.02	319.747 ± 0.67	330.97 ± 0.67	338.522 ± 0.68
	Tsallis	2.76	163 ± 3.995	137.52 ± 3.839	111.22 ± 4.113
		5.02	176.101 ± 1.049	148.433 ± 0.775	117.75 ± 0.640
	Unified function	2.76	393.535 ± 44.567	311.339 ± 77.432	296.085 ± 215.735
		5.02	407.448 ± 3.322	369.097 ± 18.529	329.4 ± 34.236
T_{kin} (MeV)	BW	2.76	124.25 ± 67.877	163.18 ± 1.700	157.73 ± 11.591
		5.02	113.571 ± 14.841	157.637 ± 4.268	164.249 ± 1.847
	TBW	2.76	76.983 ± 5.939	52.006 ± 6.026	21.143 ± 20.156
		5.02	—	76.292 ± 1.062	44.363 ± 1.163
q	Tsallis	2.76	1.0945 ± 0.0027	1.1186 ± 0.0029	1.138 ± 0.0034
		5.02	1.09736 ± 0.00072	1.12023 ± 0.00057	1.1416 ± 0.00052
	TBW	2.76	1.0135 ± 0.0102	1.0548 ± 0.0088	1.0967 ± 0.0178
		5.02	—	1.04678 ± 0.00231	1.08609 ± 0.00147
	q-Weibull	2.76	1.0212 ± 0.0141	1.0613 ± 0.0166	1.0905 ± 0.0218
		5.02	1.00274 ± 0.00409	1.04755 ± 0.00346	1.08525 ± 0.00359
	Unified function	2.76	1.0478 ± 0.0038	1.0935 ± 0.0084	1.1325 ± 0.0312
		5.02	1.04808 ± 0.00018	1.08476 ± 0.00177	1.1315 ± 0.00317
χ^2/NDF	BG	2.76	25.345	29.819	24.0907
		5.02	396.783	735.272	1080.25
	Tsallis	2.76	1.994	1.1226	0.51061
		5.02	34.3003	36.3687	23.6161
	BW	2.76	0.296	0.603	0.525
		5.02	2.08721	12.0452	20.6522
	TBW	2.76	0.666	0.515	0.351
		5.02	—	4.74803	1.74155
	q-Weibull	2.76	0.11	0.059	0.018
		5.02	1.41606	2.19311	1.15846
	Unified function	2.76	0.101	0.052	0.017
		5.02	1.70914	1.96482	1.08821

We also tried to fit this data with a statistical model as proposed in Ref. [27]. The q-Weibull distribution is an extension of Weibull distribution, which was described by Swedish mathematician Waloddi Weibull in 1951. Weibull distribution is a continuous probability distribution and is given as

$$P(x, \lambda, k) = \begin{cases} \frac{k}{\lambda}\left(\frac{x}{\lambda}\right)^{k-1} e^{-(x/\lambda)^k}, & x \geq 0, \\ 0, & x < 0, \end{cases} \quad (9)$$

where λ is the scale parameter and k is the shape parameter of distribution, with $k\&\lambda > 0$.

Weibull distribution finds its application in the system where dynamical evolution is driven by fragmentation and sequential branching [28, 29]. Since the evolution of the system in hadrons and heavy-ion collision is dominated by a perturbative QCD-based parton cascade model, we can apply q-Weibull distribution to study particle spectra.

Incorporating the Tsallis framework in Weibull distribution gives us the q-Weibull distribution [27]:

$$P_q(x, q, \lambda, k) = \frac{k}{\lambda}\left(\frac{x}{\lambda}\right)^{k-1} e_q^{-(x/\lambda)^k}, \quad (10)$$

where

$$e_q^{-(x/\lambda)^k} = \left(1 - (1-q)\left(\frac{x}{\lambda}\right)^k\right)^{(1/1-q)}. \quad (11)$$

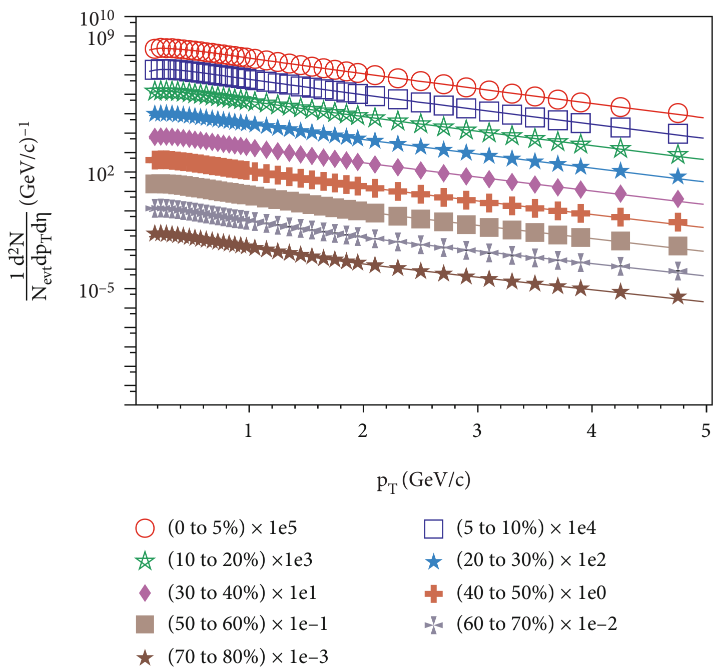

Figure 3: The transverse momentum spectra of charged hadrons at different centralities produced at collision energies of 5.02 TeV [5] fitted with Blast-Wave function (Equation (6)).

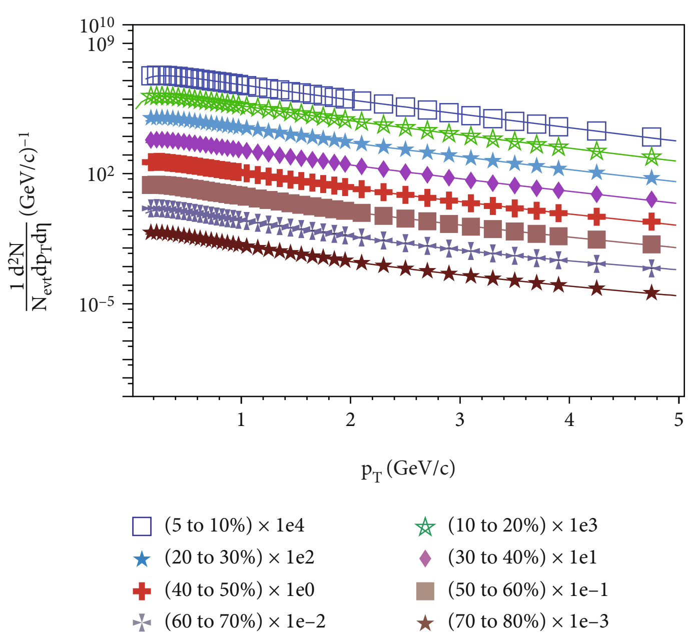

Figure 4: The transverse momentum spectra of charged hadrons at different centralities produced at collision energies of 5.02 TeV [5] fitted with Tsallis Blast-Wave function (Equation (8)).

In Figure 5, we have performed q-Weibull fit to the transverse momentum spectra data, and the fit shows good agreement with the data. Its relevance in particle spectra lies in its ability to fit spectra over a wide range of p_T as compared to the other models described above with good accuracy. The models discussed so far mostly described the data at low p_T quite well as they do not include the hard QCD processes in their construction. In the next section, we will discuss a unified formalism that describes both soft and hard processes in a consistent manner.

2.5. Unified Distribution Function. Pearson distribution is a generalized probability distribution, which, under different limits on its parameter, reduces to different distribution functions like

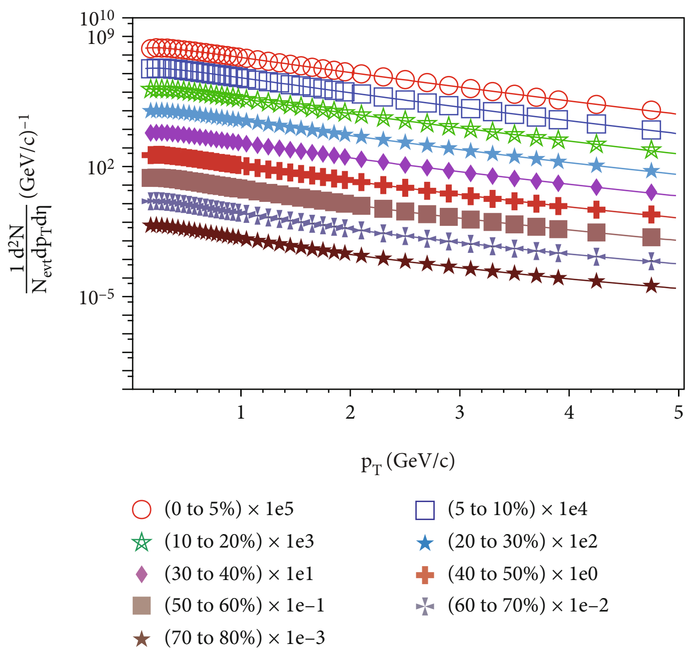

Figure 5: The transverse momentum spectra of charged hadrons at different centralities produced at collision energies of 5.02 TeV [5] fitted with q-Weibull function (Equation (10)).

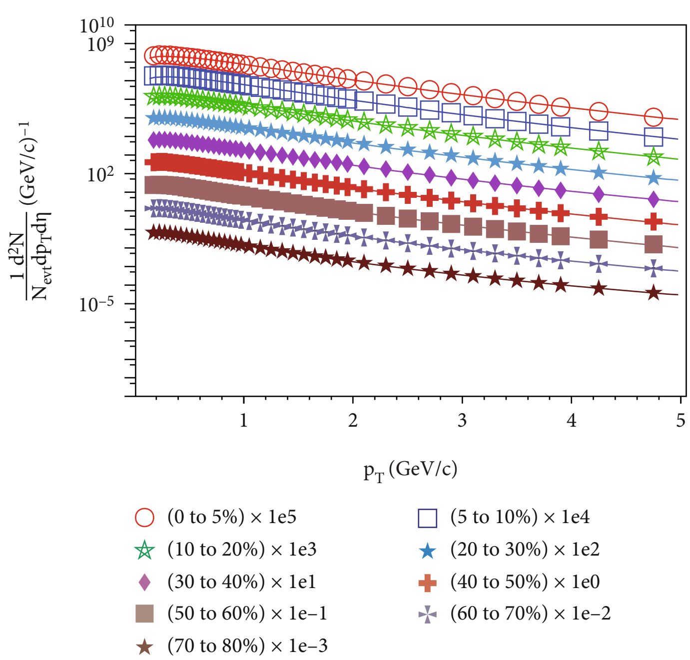

Figure 6: The transverse momentum spectra of charged hadrons at different centralities produced at collision energies of 5.02 TeV [5] fitted with unified distribution function.

exponential, Gaussian, Gamma distribution, and Student's t-distribution. It was introduced in 1895 by Karl Pearson in his seminal work [30]. It has been applied quite successfully in different fields such as geophysics, statistics, and financial marketing. It has been introduced in the context of particle production in heavy-ion collision for the first time in Ref. [24].

The transverse momentum spectra in the case of unified distribution are given as

$$\frac{1}{2\pi p_T} \frac{d^2N}{dp_T dy} = B' \left(1 + \frac{p_T}{p_0}\right)^{-n} \left(1 + (q-1)\frac{p_T}{T}\right)^{-q/q-1}. \quad (12)$$

Table 2: The best fit value of exponent "n" and average transverse flow velocity obtained by fitting the charged hadron transverse momentum spectra using BW and TBW models.

Centrality	n (BW)		$\langle\beta_T\rangle$ (BW)		$\langle\beta_T\rangle$ (TBW)	
	2.76 TeV	5.02 TeV	2.76 TeV	5.02 TeV	2.76 TeV	5.02 TeV
0 to 5%	1.2633 ± 0.7737	0.9471 ± 0.1236	0.5544 ± 0.1442	0.6303 ± 0.0291	0.4241 ± 0.0048	—
5 to 10%	1.3660 ± 0.6137	0.9538 ± 0.1322	0.534 ± 0.1059	0.6316 ± 0.0308	0.4244 ± 0.0048	0.4181 ± 0.0014
10 to 20%	1.5316 ± 1.6441	0.9740 ± 0.1465	0.5047 ± 0.2528	0.6302 ± 0.0334	0.4247 ± 0.0052	0.4192 ± 0.0013
20 to 30%	1.8038 ± 0.5546	1.1591 ± 0.1704	0.4642 ± 0.0714	0.5862 ± 0.0338	0.4254 ± 0.0052	0.4186 ± 0.0014
30 to 40%	2.1756 ± 0.4673	1.4738 ± 0.2004	0.4199 ± 0.0487	0.5225 ± 0.0319	0.4263 ± 0.0054	0.4199 ± 0.0012
40 to 50%	2.6499 ± 0.4699	1.9766 ± 0.0814	0.3771 ± 0.0389	0.4479 ± 0.0095	0.4281 ± 0.0048	0.4189 ± 0.0014
50 to 60%	3.1212 ± 0.4993	2.4192 ± 0.0799	0.3446 ± 0.0341	0.4033 ± 0.0075	0.4305 ± 0.0051	0.4200 ± 0.0016
60 to 70%	3.6574 ± 0.5502	3.2153 ± 0.0877	0.3149 ± 0.0309	0.3424 ± 0.0054	0.4330 ± 0.0052	0.4209 ± 0.0016
70 to 80%	3.9250 ± 0.5907	3.4730 ± 0.0797	0.3041 ± 0.0305	0.3301 ± 0.0048	0.4355 ± 0.0083	0.4257 ± 0.0013

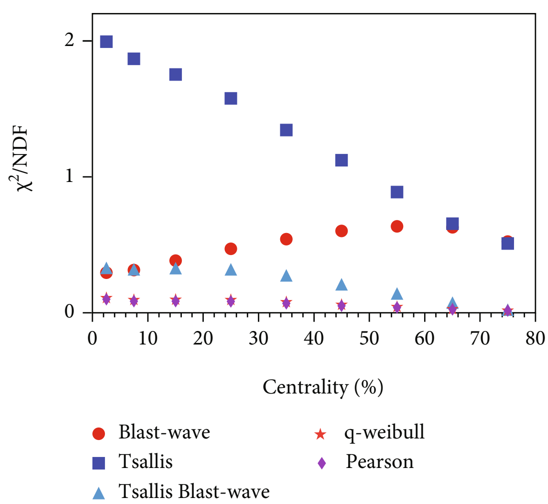

Figure 7: Value of χ^2/NDF obtained for different functions fitted with p_T spectra data of particles produced at 2.76$PbPb$ collision.

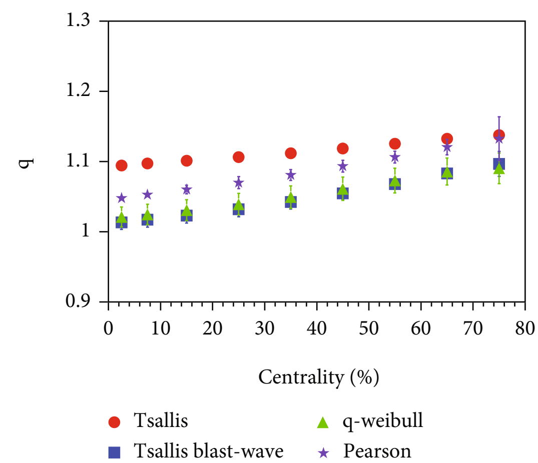

Figure 9: Value of nonextensivity parameter "q" for different functions fitted with p_T spectra data of particles produced at 2.76 TeV $PbPb$ collision.

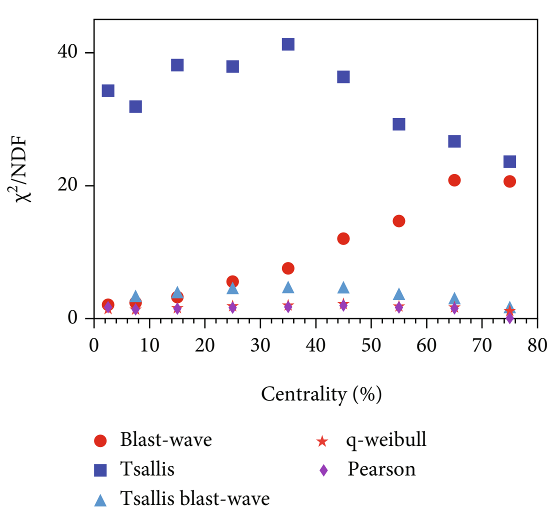

Figure 8: Value of χ^2/NDF obtained for different functions fitted with p_T spectra data of particles produced at 5.02$PbPb$ collision.

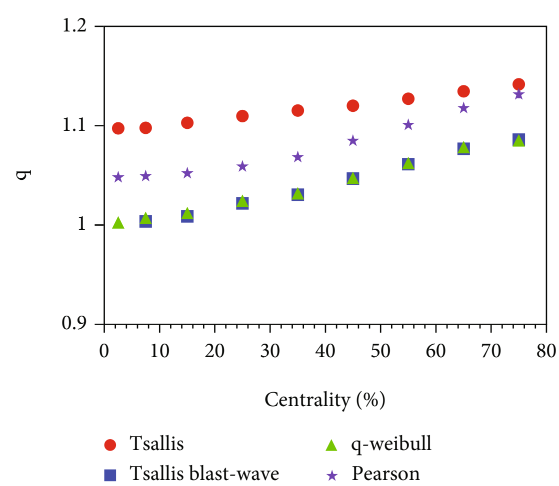

Figure 10: Value of nonextensivity parameter "q" for different functions fitted with p_T spectra data of particles produced at 5.02 TeV $PbPb$ collision.

Table 3: The best fit value of parameters k and λ obtained by fitting the charged hadron transverse momentum spectra using q-Weibull model.

Centrality	k		λ	
	2.76 TeV	5.02 TeV	2.76 TeV	5.02 TeV
0 to 5%	0.8183 ± 0.0481	0.7666 ± 0.0127	0.1953 ± 0.0170	0.1974 ± 0.0049
5 to 10%	0.8218 ± 0.0493	0.7741 ± 0.0132	0.1949 ± 0.0172	0.1988 ± 0.0049
10 to 20%	0.8297 ± 0.0503	0.7788 ± 0.0118	0.1940 ± 0.0172	0.1972 ± 0.0044
20 to 30%	0.8407 ± 0.0520	0.7998 ± 0.0115	0.1910 ± 0.0171	0.1968 ± 0.0040
30 to 40%	0.8545 ± 0.0546	0.8035 ± 0.0110	0.1865 ± 0.0172	0.1894 ± 0.0037
40 to 50%	0.8684 ± 0.0574	0.8295 ± 0.0111	0.1791 ± 0.0171	0.1853 ± 0.0035
50 to 60%	0.8816 ± 0.0621	0.8492 ± 0.0119	0.1703 ± 0.0175	0.1772 ± 0.0035
60 to 70%	0.8971 ± 0.0690	0.8717 ± 0.0156	0.1611 ± 0.0182	0.1678 ± 0.0032
70 to 80%	0.8909 ± 0.0783	0.8662 ± 0.0123	0.1489 ± 0.0197	0.1536 ± 0.0033

As it has been described in Ref. [24, 25], this form of p_T distribution function nicely takes care of both the "hard" and "soft" parts of the spectra. Further, the unified formalism also provides a connection to the flow of particle as discussed in Ref. [24].

Figure 6 represents a good agreement between transverse momentum spectra and the unified distribution function in the form of Equation (12). Apart from providing the best fit to the transverse momentum spectra (as is evident from the χ^2/NDF values provided in Table 1), unified distribution is also more physical in the sense that it is thermodynamically consistent [25], and it is also proved to be backward compatible with Tsallis distribution under limiting conditions.

3. Result

We have performed the fitting of transverse momentum spectra using different p_T distribution functions like the Boltzmann-Gibbs function, Tsallis distribution function, Blast-Wave, Tsallis Blast-Wave, and q-Weibull and unified framework. We have used the recently released p_T spectra data of charged hadrons produced in $PbPb$ collision at 5.02 TeV measured by ALICE experiment [5]. For comparison, we have also performed a similar analysis on the charged hadrons p_T spectra data produced in 2.76 TeV $PbPb$ collision [6].

In the above section, we have provided the fitting plot for 5.02 TeV p_T spectra data. Fitting has been carried out for different collision centrality classes including 0-5% (most central collision), 40-50% (midcentral collision), and 70-80% (peripheral collision). We have used the ROOT [31] data analysis framework to perform the fittings.

In Tables 1 and 2 along with Figures 7–10, best fit values of different parameters are presented along with the χ^2/NDF value which is a measure of the goodness of fit.

Looking at the q values, we can predict the nonextensivity in the system, or, in other words, we can quantify how much a system deviates from the equilibrium. Large q values indicate a nonequilibrium system, and the system approaches equilibrium as the q value approaches unity.

From Table 1, q values from all four methods, Tsallis, TBW, q-Weibull, and unified function show a decreasing trend as we move from most peripheral to most central collision indicating that the system is highly nonequilibrium in the peripheral collision, and it moves toward equilibrium as the overlap region between two colliding nuclei increases. The trend in this result shows a similar pattern reported previously for different energies in Ref. [3, 4, 27].

Table 2 shows a decreasing trend in the value of average transverse flow velocity estimated by the BW model as we go from central to peripheral collision. The corresponding numerical values for TBW fit do not show any centrality dependence, and also, the values are lower as compared to the BW model. This difference can be attributed to the absence of the nonequilibrium description in the BW model as it demands the system to be in thermal equilibrium.

Apart from the nonextensivity parameter, the q-Weibull fit also provides the value of two more free parameters λ and k. The best fit value of these parameters is presented in Table 3. The value of parameter k increases as we go from central to peripheral collision for both the energies. The values are also consistently higher in 2.76 TeV as compared to the 5.02 TeV. The parameter λ shows a reverse trend with the values decreasing from central to peripheral collision. The physics interpretation of these parameters is still an open problem, and a detailed study of q-Weibull function is required to have a better understanding of the model.

Among all the different distribution functions, we have obtained the best fit for the unified distribution, which is also evident from the χ^2/NDF values. One possible reason for the low χ^2/NDF in unified distribution as compared to other distributions is that it also takes care of hard perturbative QCD processes, which affect the p_T distribution at higher p_T range as described in Ref. [24]. Another interesting result which is underdiscussed is related to the scaling properties of q parameter. Since the q parameter acts as a scaling factor to apply statistical mechanics at the low number of particles, the number of final state particles decreases with the increase in centrality, and hence, the corresponding scaling parameter should increase with centrality. We observe this in Figures 9 and 10 for all four different methods indicating that the q parameter can be interpreted as a scaling factor depending upon the number of final state particles in the system.

4. Conclusion

In this work, we have analyzed the p_T spectra of charged particles produced in $PbPb$ collision at $\sqrt{s_{NN}} = 5.02\,\text{TeV}$ using six different formalisms which are based on different physics inputs; for example, Boltzmann distribution is a purely thermal model, Blast-Wave models also include collective flow effect, and the unified distribution also takes into account hard QCD processes. The effects such as nonextensivity and collective flow need to be taken into account in a model for explaining such data. From the variation of q -parameter with centrality, we also observe that the system is highly nonequilibrium at the peripheral collision and moves toward the equilibrium as we move toward the most central collision. Further, a very high value of χ^2/NDF indicates that a purely thermal model is not a good explanation for the p_T spectra. Apart from this, the scaling properties of the q parameter have also been established, indicating its relevance in small systems.

In conclusion, we can say that a complete model to explain transverse momentum spectra must include the nonextensivity and collective flow on top of random thermal motion and should also be able to explain the effects on high p_T range arising due to hard pQCD processes. The essence of all these physics inputs is present in the unified distribution, and it also provides the best fit to the transverse momentum spectra as is evident from the values of χ^2/NDF presented in Figures 7 and 8.

Data Availability

The data used for this analysis are already published and are cited at relevant places within the text as references.

Disclosure

The preprint of this paper has been previously uploaded to arxiv [32].

Conflicts of Interest

The authors declare that they have no known competing financial interests or personal relationships that could have appeared to influence the work reported in this paper.

Acknowledgments

R. Gupta would like to acknowledge the financial support provided by CSIR through fellowship number 09/947 (0067) 2015-EMR-1.

References

[1] L. Stodolsky, "Temperature fluctuations in multiparticle production," *Physical Review Letters*, vol. 75, pp. 1044-1045, 1995.

[2] C. Tsallis, "Possible generalization of Boltzmann-Gibbs statistics," *Journal of Statistical Physics*, vol. 52, no. 1-2, pp. 479–487, 1988.

[3] O. Ristea, A. Jipa, C. Ristea et al., "Study of the freeze-out process in heavy ion collisions at relativistic energies," *Journal of Physics Conference Series*, vol. 420, article 012041, 2013.

[4] Z. Tang, Y. Xu, L. Ruan, G. van Buren, F. Wang, and Z. Xu, "Spectra and radial flow in relativistic heavy ion collisions with Tsallis statistics in a blast-wave description," *Physical Review C*, vol. 79, no. 5, article 051901, 2009.

[5] The ALICE Collaboration, "Transverse momentum spectra and nuclear modification factors of charged particles in pp, p-Pb and Pb-Pb collisions at the LHC," *Journal of High Energy Physics*, vol. 2018, no. 11, 2018.

[6] B. Abelev, J. Adam, D. Adamová et al., "Centrality dependence of charged particle production at large transverse momentum in Pb-Pb collisions at sNN=2.76 TeV," *Physics Letters B*, vol. 720, no. 1-3, pp. 52–62, 2013.

[7] H. Koppe and Z. Naturforschg, "Die Mesonenausbeute beim Beschuß von leichten Kernen mit x-Teilchen," *Zeitschrift für Naturforschung A*, vol. 3, no. 4, pp. 251-252, 1948.

[8] A. N. Tawfik, "Koppe's work of 1948: a fundamental for non-equilibrium rate of particle production," *Zeitschrift für Naturforschung A*, vol. 69, no. 1-2, pp. 106-107, 2014.

[9] E. Fermi, "High energy nuclear events," *Progress in Theoretical Physics*, vol. 5, no. 4, pp. 570–583, 1950.

[10] E. Fermi, "Angular distribution of the pions produced in high energy nuclear collisions," *Physics Review*, vol. 81, no. 5, pp. 683–687, 1951.

[11] R. Hagedorn, "Statistical thermodynamics of strong interactions at high-energies," *Supplemento al Nuovo Cimento*, vol. 3, p. 147, 1965.

[12] R. Hagedorn and J. Ranft, "Statistical thermodynamics of strong interactions at high-energies. 2. Momentum spectra of particles produced in pp-collisions," *Supplemento al Nuovo Cimento*, vol. 6, p. 169, 1968.

[13] E. Schnedermann, J. Sollfrank, and U. W. Heinz, "Thermal phenomenology of hadrons from 200AGeV S+S collisions," *Physical Review C*, vol. 48, no. 5, pp. 2462–2475, 1993.

[14] J. Cleymans and D. Worku, "Relativistic thermodynamics: transverse momentum distributions in high-energy physics," *European Physical Journal A: Hadrons and Nuclei*, vol. 48, no. 11, p. 160, 2012.

[15] G. Wilk and Z. Wlodarczyk, "Application of nonextensive statistics to particle and nuclear physics," *Physica A*, vol. 305, no. 1-2, pp. 227–233, 2002.

[16] G. Wilk and Z. Wlodarczyk, "Consequences of temperature fluctuations in observables measured in high-energy collisions," *European Physical Journal A: Hadrons and Nuclei*, vol. 48, no. 11, p. 161, 2012.

[17] J. Cleymans and D. Worku, "The Tsallis distribution in proton–proton collisions at $\sqrt{s}$ = 0.9 TeV at the LHC," *Journal of Physics G: Nuclear and Particle Physics*, vol. 39, no. 2, article 025006, 2012.

[18] A. Khuntia, S. Tripathy, R. Sahoo, and J. Cleymans, "Multiplicity dependence of non-extensive parameters for strange and multi-strange particles in proton-proton collisions at $\sqrt{s} = 7$ TeV at the LHC," *European Physical Journal A: Hadrons and Nuclei*, vol. 53, no. 5, p. 103, 2017.

[19] S. Abe and Y. Okamoto, *Nonextensive Statistical Mechanics and Its Applications*, Springer Science & Business Media, 2001.

[20] C. Tsallis, *Introduction to Nonextensive Statistical Mechanics*, Springer, New York, NY, USA, 2009.

[21] C. Y. Wong and G. Wilk, "Tsallis fits to p T spectra and multiple hard scattering in p p collisions at the LHC," *Physical Review D*, vol. 87, no. 11, article 114007, 2013.

[22] K. Saraswat, P. Shukla, V. Singh, and J. Phys, "Transverse momentum spectra of hadrons in high energy pp and heavy ion collisions," *Journal of Physics Communications*, vol. 2, no. 3, article 035003, 2018.

[23] M. D. Azmi and J. Cleymans, "The Tsallis distribution at large transverse momenta," *The European Physical Journal C*, vol. 75, no. 9, p. 430, 2015.

[24] S. Jena and R. Gupta, "A unified formalism to study transverse momentum spectra in heavy-ion collision," *Physics Letters B*, vol. 807, article 135551, 2020.

[25] R. Gupta, A. Menon, and S. Jena, *A generalised thermodynamical approach to transverse momentum spectra in high energy collision*, 2020.

[26] S. Basu, R. Chatterjee, B. K. Nandi, and T. K. Nayak, "Characterization of relativistic heavy-ion collisions at the Large Hadron Collider through temperature fluctuations," https://arxiv.org/abs/1504.04502.

[27] S. Dash and D. Mahapatra, "pT spectra in pp and AA collisions at RHIC and LHC energies using the Tsallis-Weibull approach," *European Physical Journal A: Hadrons and Nuclei*, vol. 54, no. 4, pp. 1–9, 2018.

[28] W. K. Brown, "A theory of sequential fragmentation and its astronomical applications," *Journal of Astrophysics and Astronomy*, vol. 10, no. 1, pp. 89–112, 1989.

[29] W. K. Brown and K. H. Wohletz, "Derivation of the Weibull distribution based on physical principles and its connection to the Rosin–Rammler and lognormal distributions," *Journal of Applied Physics*, vol. 78, no. 4, pp. 2758–2763, 1995.

[30] K. Pearson, "Philosophical transactions of the Royal Society of London a: mathematical," *Physical and Engineering Sciences*, vol. 186, p. 343, 1895.

[31] R. Brun and F. Rademakers, "ROOT – an object oriented data analysis framework," *Nuclear Instruments and Methods in Physics Research Section A: Accelerators, Spectrometers, Detectors and Associated Equipment*, vol. 389, pp. 81–86, 1997.

[32] R. Gupta and S. Jena, "Model comparison of the transverse momentum spectra of charged hadrons produced in *PbPb* collision at $\sqrt{s_{NN}} = 5.02$ TeV," https://arxiv.org/abs/2103.13104.